B anomalies in the post-$R_{K^{(*)}}$ era

T. Hurth,[1] F. Mahmoudi,[2,3,4] and S. Neshatpour[2,5]

[1]*PRISMA+ Cluster of Excellence and Institute for Physics (THEP), Johannes Gutenberg University, D-55099 Mainz, Germany*
[2]*Université de Lyon, Université Claude Bernard Lyon 1, CNRS/IN2P3, Institut de Physique des 2 Infinis de Lyon, UMR 5822, F-69622 Villeurbanne, France*
[3]*CERN, Theoretical Physics Department, CH-1211 Geneva 23, Switzerland*
[4]*Institut Universitaire de France (IUF), 75005 Paris, France*
[5]*INFN-Sezione di Napoli, Complesso Universitario di Monte S. Angelo, Via Cintia Edificio 6, 80126 Napoli, Italy*

(Received 17 October 2023; accepted 4 December 2023; published 27 December 2023)

We discuss the status of $b \to s\ell^+\ell^-$ decays in the post-$R_{K^{(*)}}$ era. The recent LHCb update of R_K and R_{K^*} measurements, which are now compatible with the Standard Model, constrain new physics contributions to be lepton-flavor universal, allowing only small deviations from this limit. In addition to the latest LHCb measurements of R_K and R_{K^*}, we also include the recent CMS measurements of R_K and of the branching ratio of $B^+ \to K^+\mu^+\mu^-$. We present a model-independent analysis of the $b \to s\ell^+\ell^-$ data and investigate the implications of the different sets of observables. In addition, we consider multidimensional fits and discuss the significance of more complex new physics scenarios compared to one- and two-dimensional scenarios.

DOI: 10.1103/PhysRevD.108.115037

I. INTRODUCTION

Over the last nine years, the LHCb Collaboration reported hints for lepton nonuniversality at the 3σ level via measurements of the ratios R_K and R_{K^*} (see Refs. [1,2] and references therein). The R_K and R_{K^*}, which are defined as the ratios of the branching fractions of $B \to K^{(*)}\ell^+\ell^-$ for muons vs electrons, are theoretically very clean, with uncertainties of less than 1% and central values close to unity in the Standard Model (SM) due to the universality of the lepton flavors [3,4]. In addition, there are long-standing tensions in the angular observables and branching ratios of exclusive $b \to s$ observables [5–13]. The initial indication of tensions arose in one of the low-q^2 bins within the angular observable $P_5'(B \to K^*\mu^+\mu^-)$ [5], which could potentially be explained by introducing new physics contributions to C_9 [14–18]. This interpretation was reinforced, as the same new physics effect could also account for inconsistencies in other exclusive $b \to s$ decays. However, in general, the observables of the exclusive decays are dependent on local matrix elements (form factors), as well as nonlocal ones, which often make it difficult to distinguish between possible new physics effects and hadronic effects. Although some of the angular observables are less sensitive to the form factors, they do depend on nonlocal hadronic contributions, which are not well known. The significance of the anomalies in exclusive decays is therefore dependent on the estimated size of the nonlocal effects. Recent theoretical progress in the evaluation of the nonlocal contributions [19–21] indicate that the nonfactorizable power corrections are small. The crucial point of the previous situation was that the deviations in the theoretically clean ratios on one side and in the angular observables and branching ratios on the other side could be consistently described with the same new physics scenarios; this was noted [22–31] after the first LHCb measurement [32] of R_K in 2014 and confirmed by subsequent studies [33–39] with the first measurement of R_{K^*} by LHCb [1] in 2017 (see also [40–55] for later studies). This consistency was again increased with the updated measurement of $\mathrm{BR}(B_s \to \mu^+\mu^-)$ from last year [56]. The combination of this result with the ATLAS and LHCb measurements [57–59] $\mathrm{BR}(B_s \to \mu^+\mu^-)^{\mathrm{comb}}_{\mathrm{exp}} = (3.52^{+0.32}_{-0.30}) \times 10^{-9}$ as given in [60] is in agreement with the SM within 1σ, suppressing large new physics contributions in the Wilson coefficient C_{10}. However, the LHCb Collaboration recently presented new measurements of the ratios that turn out to be compatible with the Standard Model [61],

Published by the American Physical Society under the terms of the Creative Commons Attribution 4.0 International license. Further distribution of this work must maintain attribution to the author(s) and the published article's title, journal citation, and DOI. Funded by SCOAP³.

$$\begin{cases} R_K([0.1-1.1]) = 0.994^{+0.090+0.029}_{-0.082-0.027}, \\ R_K([1.1-6.0]) = 0.949^{+0.042+0.022}_{-0.041-0.022}, \end{cases} \qquad \begin{cases} R_{K^*}([0.1-1.1]) = 0.927^{+0.093+0.036}_{-0.087-0.035}, \\ R_{K^*}([1.1-6.0]) = 1.027^{+0.072+0.027}_{-0.068-0.026}. \end{cases}$$

In this paper, we analyze the current situation in a model-independent way. Clearly, the tensions in the angular observables and branching ratios are untouched by the new LHCb measurements. We analyze the two sets of $b \to s$ data separately, namely, the theoretically clean ratios together with BR($B_{s,d} \to \ell^+\ell^-$) on one side and the angular observables and branching ratios on the other side.

We also include the very recent measurements of R_K and the branching ratio of $B^+ \to K^+\mu^+\mu^-$ by the CMS Collaboration [62], which both turn out to be compatible with the SM predictions. In addition, we update the Cabibbo-Kobayashi-Maskawa (CKM) parameters where we have updated the PDG 2020 [63] values to PDG 2022 [64], with the old and new inputs given as follows:

	λ	A	$\bar\rho$	$\bar\eta$
PDG (2020)	0.22650 ± 0.00048	$0.790^{+0.017}_{-0.012}$	$0.141^{+0.016}_{-0.017}$	0.357 ± 0.011
PDG (2022)	0.22500 ± 0.00067	$0.826^{+0.018}_{-0.015}$	0.159 ± 0.010	0.348 ± 0.010

The complete list of the observables used in the present fits can be read off the corresponding list in our previous analysis in Refs. [55,60]. For our analysis we have used the SuperIso public program [65–69] assuming 10% uncertainty for the unknown nonfactorizable power corrections (see Ref. [31] for more details). For other global analyses with the updated LHCb measurement of $R_{K^{(*)}}$ (not including the recent CMS measurement), see, for example, [70–73].

This paper is organized as follows: In the next section, we show the one- and two-dimensional fits for different sets of observables. In Sec. II A we consider clean observables and discuss the impact of the new LHCb measurement for the ratios, and in Sec. II B the fit to the rest of the observables is given, where the impact from the CMS measurement on BR ($B^+ \to K^+\mu^+\mu^-$) as well as the updated CKM values are visible. In Sec. II C the fit to all $b \to s$ data are given and the impact of various sets of observables are discussed. Section III includes a 12-dimensional fit and shows via the Wilks test that beyond C_9 adding further degrees of freedom only improves the fit marginally. Finally, we summarize in Sec. IV.

TABLE I. One operator NP fit to clean observables before and after update of $R_{K^{(*)}}$ by the LHCb Collaboration.

Only LFUV ratios and $B_{s,d} \to \ell^+\ell^-$ pre-$R_{K^{(*)}}$ update ($\chi^2_{\rm SM} = 30.63$)			
	Best-fit value	$\chi^2_{\rm min}$	Pull$_{\rm SM}$
δC_9^e	0.83 ± 0.21	10.8	4.4σ
δC_9^μ	-0.80 ± 0.21	11.8	4.3σ
δC_{10}^e	-0.81 ± 0.19	8.7	4.7σ
δC_{10}^μ	0.50 ± 0.14	16.2	3.8σ
$\delta C_{\rm LL}^e$	0.43 ± 0.11	9.7	4.6σ
$\delta C_{\rm LL}^\mu$	-0.33 ± 0.08	12.4	4.3σ
Only LFUV ratios and $B_{s,d} \to \ell^+\ell^-$ post-$R_{K^{(*)}}$ update ($\chi^2_{\rm SM} = 9.37$)			
	Best-fit value	$\chi^2_{\rm min}$	Pull$_{\rm SM}$
δC_9^e	0.17 ± 0.16	8.2	1.1σ
δC_9^μ	-0.18 ± 0.16	8.1	1.1σ
δC_{10}^e	-0.15 ± 0.14	8.3	1.1σ
δC_{10}^μ	0.15 ± 0.12	7.7	1.3σ
$\delta C_{\rm LL}^e$	0.08 ± 0.08	8.2	1.1σ
$\delta C_{\rm LL}^\mu$	-0.09 ± 0.07	7.7	1.3σ

II. ONE- AND TWO-DIMENSIONAL FITS

A. Fits to clean $b \to s\ell\ell$ observables

First, we analyze the significance of new physics (NP) within the clean observables, $R_{K^{(*)}}$ and BR$(B_{s,d} \to \mu^+\mu^-)$. In Table I we show the one-operator fits to these clean observables, both before[1] and after the latest $R_{K^{(*)}}$ measurements. The change is a drastic one, as only small deviations from lepton universality are now allowed. There are still lepton-flavor universality violating (LFUV) ratios, namely, $R^{\rm LHCb}_{K^0_S}([1.1-6.0])$, $R^{\rm LHCb}_{K^{*+}}([0.045-6.0])$ [74] and $R^{\rm LHCb}_{K}([1.1-6.0])$ [61] with 1.7, 1.4, and 1.1σ NP significance, respectively.[2]

[1]In this paper, pre-$R_{K^{(*)}}$ indicates the fit to the data before the LHCb update on $R_{K^{(*)}}$ as given in [60].

[2]A reanalysis of $R^{\rm LHCb}_{K^0_S}([1.1-6.0])$ and $R^{\rm LHCb}_{K^{*+}}([0.045-6.0])$ regrading possible misidentifications would not change the NP significances much given the large experimental uncertainties [75].

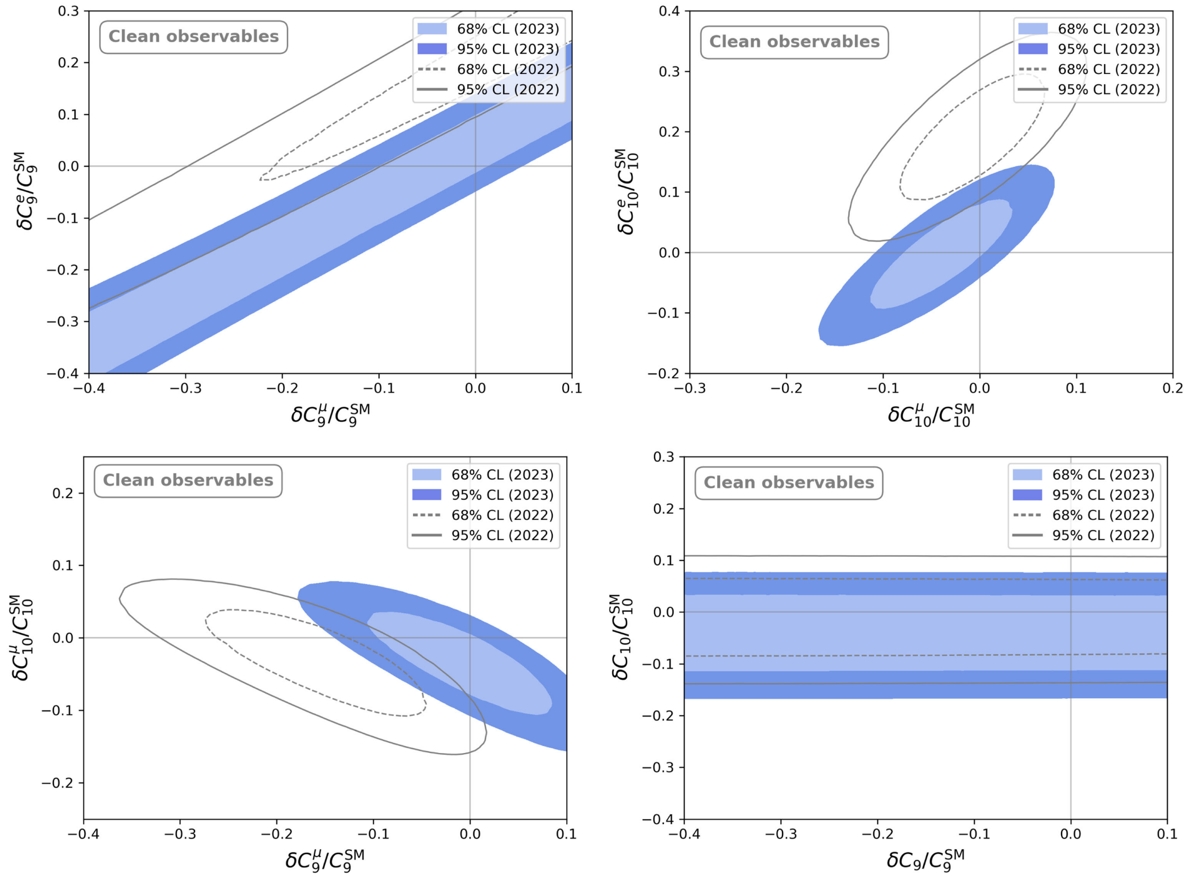

FIG. 1. Two-dimensional fits to clean observables. The colored regions correspond to the post-$R_{K^{(*)}}$ fits and the gray contours correspond to the fits prior to the recent $R_{K^{(*)}}$ update [60].

The corresponding two-operator fits are shown in Fig. 1. The two upper plots clearly show that the new data confirm lepton universality. The 1 and 2σ regions in the case of $\{C_9^e, C_9^\mu\}$ and also in the case of $\{C_{10}^e, C_{10}^\mu\}$ are located around the diagonal. The favored regions in the case of $\{C_{10}^e, C_{10}^\mu\}$ are bounded along the diagonal because we have included $\mathrm{BR}(B_{s,d} \to \mu^+\mu^-)$ in the fit, which implies strong constraints on C_{10} in general. The lower left plot in Fig. 1 shows the two-operator fit to $\{C_9^\mu, C_{10}^\mu\}$. The 1 or 2σ regions are now also grouped around the secondary diagonal and contain the SM values. Only small NP contributions are still possible after the new measurements. We note, however, that without $\mathrm{BR}(B_{s,d} \to \mu^+\mu^-)$ in the fit, i.e., without the strong constraint on C_{10}^μ, much larger values of C_9^μ and C_{10}^μ would be possible along the secondary diagonal. Such larger contributions are then, in principle, possible, but due to unnatural cancellations of these two contributions in the ratios R_K and R_{K^*} only. The lower right plot is trivial. It shows that our set of clean observables does not constrain the universal coefficient C_9, but that $\mathrm{BR}(B_{s,d} \to \mu^+\mu^-)$ constrains the universal C_{10}. The slight shift along the C_{10} axis compared to the pre-$R_{K^{(*)}}$ fit is due to the modified SM prediction of $\mathrm{BR}(B_s \to \mu^+\mu^-)$ owing to the updated CKM inputs.

B. Fits to all $b \to s\ell\ell$ data except clean observables

In Table II we show the one-parameter fits to the rest of the $b \to s$ observables—excluding the clean observables discussed before. These fits are, of course, almost unchanged compared to the situation before the new measurements of R_K and R_{K^*}. The slight differences in the NP significance are due to the new measurements by CMS and also the update of the CKM parameters. However, the comparison of the one-operator fits to the clean observables in Table I and of those to the remaining $b \to s$ observables in Table II no longer show, for the nonuniversal Wilson coefficients C_9^μ and C_{LL}^μ, any consistency, which means that the remaining large tensions in the rest of the $b \to s$ observables, in particular, in the angular observables and in the branching ratios, should be described with lepton-universal operators; only small deviations from the lepton universality are allowed. Let us emphasize that the NP significances given in Table II are based on the assumption of 10% power corrections to the angular observables and branching ratios.

C. Fits to all $b \to s\ell\ell$ observables

This brings us to the fits to all $b \to s$ observables, where we now use lepton-universal operators only—assuming

TABLE II. One-operator fits for all except clean observables before and also after the LHCb-update of $R_{K^{(*)}}$.

All observables except LFUV ratios and $B_{s,d} \to \ell^+\ell^-$ pre-$R_{K^{(*)}}$ update ($\chi^2_{\rm SM} = 221.8$)			
	Best-fit value	$\chi^2_{\rm min}$	Pull$_{\rm SM}$
δC_9	-0.95 ± 0.13	185.1	6.1σ
δC_9^e	0.70 ± 0.60	220.5	1.1σ
δC_9^μ	-0.96 ± 0.13	182.8	6.2σ
δC_{10}	0.29 ± 0.21	219.8	1.4σ
δC_{10}^e	-0.60 ± 0.50	220.6	1.1σ
δC_{10}^μ	0.35 ± 0.20	218.7	1.8σ
$\delta C_{\rm LL}^e$	0.34 ± 0.29	220.6	1.1σ
$\delta C_{\rm LL}^\mu$	-0.64 ± 0.13	195.0	5.2σ

All observables except LFUV ratios and $B_{s,d} \to \ell\bar{\ell}$ post-$R_{K^{(*)}}$ update ($\chi^2_{\rm SM} = 261.6$)			
	Best-fit value	$\chi^2_{\rm min}$	Pull$_{\rm SM}$
δC_9	-0.97 ± 0.13	221.9	6.3σ
δC_9^e	0.70 ± 0.60	260.4	1.1σ
δC_9^μ	-0.98 ± 0.13	219.7	6.5σ
δC_{10}	0.36 ± 0.20	258.3	1.8σ
δC_{10}^e	-0.50 ± 0.50	260.5	1.0σ
δC_{10}^μ	0.41 ± 0.20	257.0	2.1σ
$\delta C_{\rm LL}^e$	0.31 ± 0.28	260.4	1.1σ
$\delta C_{\rm LL}^\mu$	-0.65 ± 0.12	231.7	5.5σ

again 10% power corrections for the angular observables and branching ratios. The results are given in Table III, where we can see that the favored universal coefficient is C_9 in order to explain the tensions in the angular observables and branching ratios. In principle, C_9^μ and C_{LL}^μ can explain the tensions, but these new physics contributions would not be compatible with the constraints induced by the clean observables as we showed above. In Table IV one-operator fits using chiral-universal coefficients[3] are shown. One finds a rather large NP significance for the fits to C_{LL} and C_{LR}, i.e., for left-handed quark currents.

In addition, we present the two-dimensional fit results in Fig. 2. The lower right plot in the $\{C_9, C_{10}\}$ plane is the crucial one. It shows that the universal coefficient C_9, not C_{10}, explains the present anomalies best. This is also a consequence of the C_{10} dependence of the $B_s \to \mu^+\mu^-$ branching ratio that is SM-like. The two-operator fits in the upper row, $\{C_9^\mu, C_9^e\}$ and $\{C_{10}^\mu, C_{10}^e\}$, essentially are again consequences of lepton-flavor universality. In both

TABLE III. One-operator NP fits to all $b \to s\ell\ell$ observables before and after the update of $R_{K^{(*)}}$ by the LHCb Collaboration.

All observables pre-$R_{K^{(*)}}$ update ($\chi^2_{\rm SM} = 253.5$)			
	Best-fit value	$\chi^2_{\rm min}$	Pull$_{\rm SM}$
δC_7	-0.02 ± 0.01	248.7	2.2σ
δC_{Q_1}	-0.05 ± 0.02	252.3	1.1σ
δC_{Q_2}	-0.01 ± 0.01	252.4	1.0σ
δC_9	-0.95 ± 0.13	215.8	6.1σ
δC_{10}	0.08 ± 0.16	253.2	0.5σ

All observables post-$R_{K^{(*)}}$ update ($\chi^2_{\rm SM} = 271.0$)			
	Best-fit value	$\chi^2_{\rm min}$	Pull$_{\rm SM}$
δC_7	-0.02 ± 0.01	267.2	1.9σ
δC_{Q_1}	-0.04 ± 0.03	270.3	0.8σ
δC_{Q_2}	-0.01 ± 0.01	270.4	0.8σ
δC_9	-0.96 ± 0.13	230.7	6.3σ
δC_{10}	0.15 ± 0.15	270.0	1.0σ

plots, the 1 and 2σ ranges have moved to the diagonal and have become thinner compared to the ones of the pre-$R_{K^{(*)}}$ measurements. Moreover, the 1σ range of the $\{C_{10}^\mu, C_{10}^e\}$ fit includes the SM values. It becomes clear that these two-operator plots essentially reproduce the one-operator fits to the corresponding universal C_9 and C_{10}. Also, the NP significance is similar as one can read off from Tables III and V.

The plot in the lower row on the left shows the two-operator fit to $\{C_9^\mu, C_{10}^\mu\}$. Compared to the pre-$R_{K^{(*)}}$ update, the 1 or 2σ ranges now move in the direction of the second diagonal to allow a partial compensation of the C_9^μ and the C_{10}^μ contributions within the $R_{K^{(*)}}$ ratios. Because of this unnatural compensation, this specific two-operator fit should be considered critical. In comparison with the corresponding plot in Fig. 1 with the fits to the clean observables, one needs now a larger C_9^μ for the explanation of the present tensions, which again indicates the present measurements are best described by flavor-universal operators.

As one can read off from Table V, all two-operator fits discussed have a large NP significance up to 6σ besides the case $\{C_{10}^\mu, C_{10}^e\}$.

Next, we will have a closer look at the 2 two-operator fits to $\{C_9^\mu, C_{10}^\mu\}$ and $\{C_9, C_{10}\}$. We consider the bounds of the $R_{K^{(*)}}$ ratios separate from the ones induced by the $B_{s,d} \to \mu^+\mu^-$ branching ratios. Likewise, in the case of the remaining $b \to s\ell^+\ell^-$ observables, we examine the impact of the low- and high-q^2 observables separately. Since the validity of soft-collinear effective theory (SCET) in the low-q^2 bin $[6, 8]$ GeV^2 (near the J/ψ resonance) is questionable, we separate this bin from the other low-q^2 bins up to 6 GeV^2.

[3]We use the standard notation C_{XY} where X denotes the chirality of the quark current and Y of the lepton one. Assuming left-handed leptons only, we have $C_{LL} \equiv C_9 = -C_{10}$ and $C_{RL} \equiv C_9' = -C_{10}'$; for right-handed leptons, $C_{RR} \equiv C_9' = C_{10}'$ and $C_{LR} \equiv C_9 = C_{10}$.

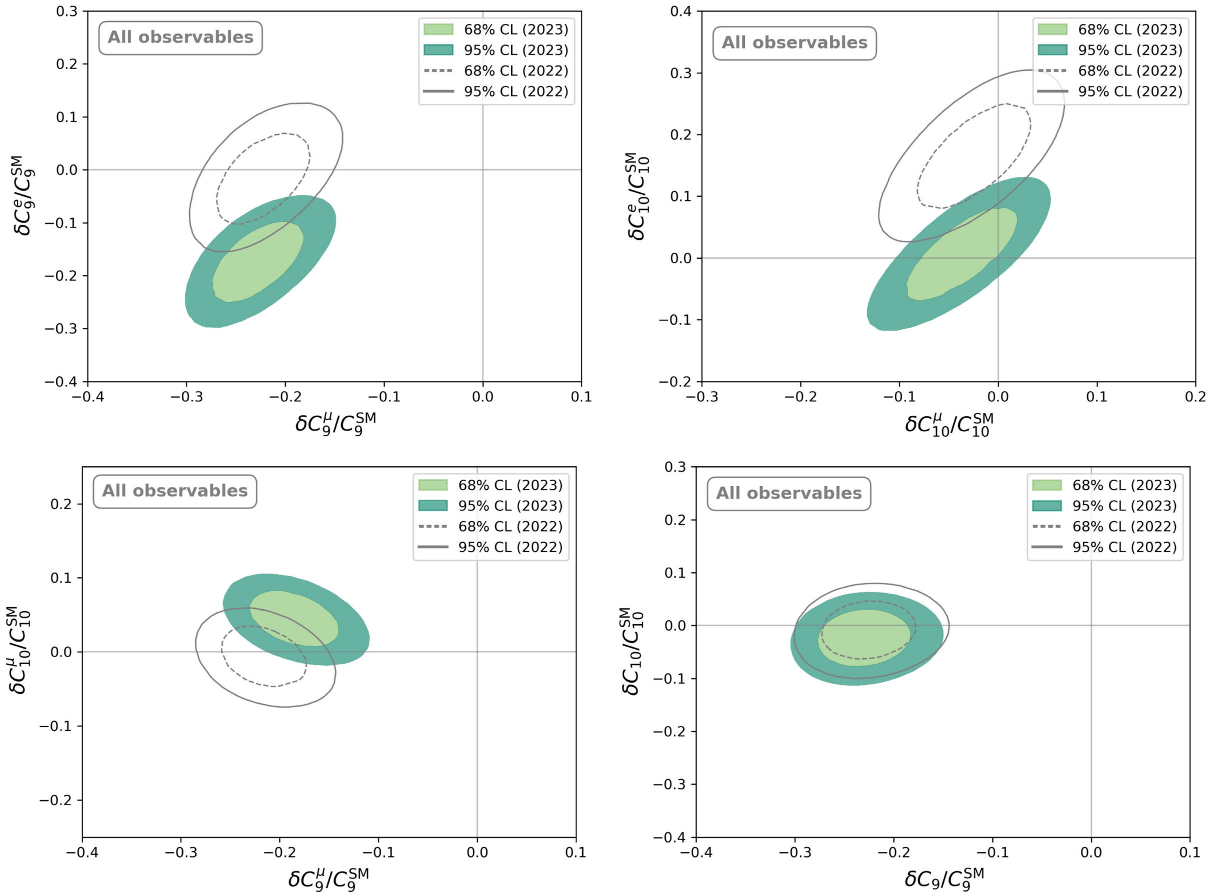

FIG. 2. Two-dimensional fits to all observables with the best-fit point given in Table V.

In Fig. 3 the two-operator fits have been dissected in order to show the impact that each of these different sets of observables have on the overall fit. In the plot on the right-hand side of Fig. 3, the $\{C_9, C_{10}\}$ two-operator fit has been shown, where the brown contours show the 1 and 2σ regions of the high-q^2 observables. It can be seen that they are compatible with the SM values with comparatively large uncertainties. The tensions in the angular observables and the branching ratios obviously have their main origin in the low-q^2 observables, as can be seen from the purple contours. It is well known that the high-q^2 observables have a weak dependence on the Wilson coefficients, which implies a low sensitivity to NP.[4] The yellow contours show that the inclusion of the highest low-q^2 bin from 6 to 8 GeV^2 in the fit massively increases the NP significance. However, it could be that this large effect just indicates that SCET is no longer valid in this range. Finally, the $B_{s,d} \to \mu^+\mu^-$ branching ratios lead to the gray contours that just bound the Wilson coefficient C_{10}.

[4]In principle, the high-q^2 observables are theoretically cleaner. There is a local operator product expansion to describe power corrections (see, i.e., Refs. [76,77]).

In the plot on the left-hand side of Fig. 3 we look at the bounds on $\{C_9^\mu, C_{10}^\mu\}$. The blue 1 and 2σ regions show the bounds generated by the ratios $R_{K^{(*)}}$. This can be compared to the lower right plot of Fig. 1, where the bound from the ratios together with $\mathrm{BR}(B_{s,d} \to \mu^+\mu^-)$ was shown. One realizes that now much larger values of C_9^μ and also of C_{10}^μ are allowed, but this is possible due to an unnatural compensation between the C_9^μ and the C_{10}^μ contributions in the ratios, which makes the $\{C_9^\mu, C_{10}^\mu\}$ fit problematic, as already mentioned above. The $B_{s,d} \to \mu^+\mu^-$ branching ratios alone bound C_{10}^μ to smaller values again, as can be seen from the gray contours.

TABLE IV. One-operator fits to all $b \to s\ell\ell$ observables in the chiral basis.

All observables post-$R_{K^{(*)}}$ update ($\chi^2_{\rm SM} = 271.0$)			
	Best-fit value	$\chi^2_{\rm min}$	Pull$_{\rm SM}$
$\delta C_{\rm LL}$	-0.54 ± 0.12	249.1	4.7σ
$\delta C_{\rm LR}$	-0.42 ± 0.10	257.4	3.7σ
$\delta C_{\rm RL}$	0.00 ± 0.08	268.8	1.5σ
$\delta C_{\rm RR}$	0.21 ± 0.13	268.1	1.7σ

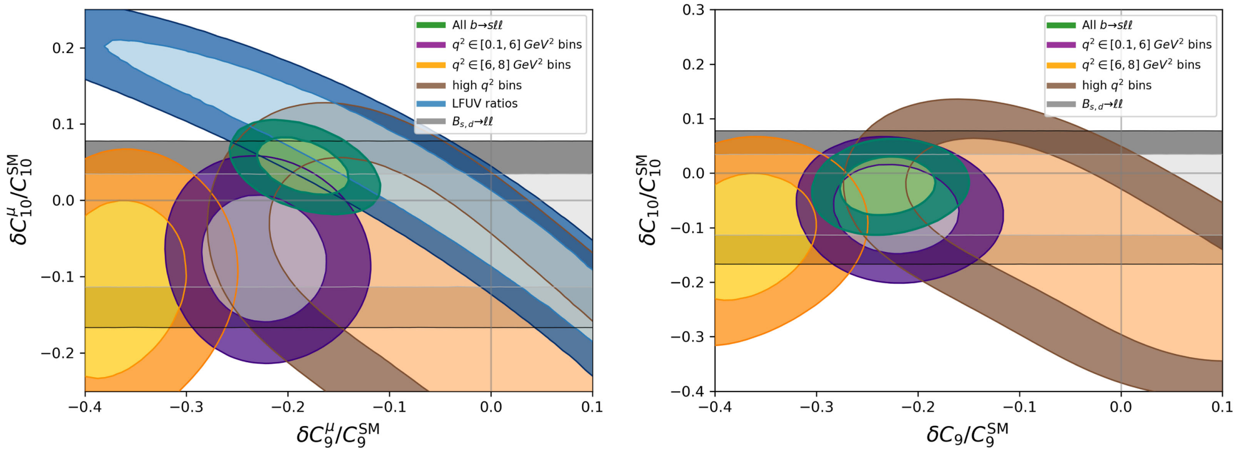

FIG. 3. Two-dimensional fits to all observables in green. Where relevant, the impact of the $b \to s\ell\ell$ observables for the low-q^2 bins up to 6 GeV^2, for the $[6, 8]$ GeV^2 bin, and for the high-q^2 bins, as well as the bounds from the lepton-flavor universality violating ratios and $B_{s,d} \to \ell^+\ell^-$ are shown separately with the lighter (darker) shade indicating the 68% (95%) confidence level region.

III. GLOBAL ANALYSES

In order to present the global analysis, we provide multidimensional fits considering only universal operators, which may be more realistic than assuming one- or two-operator fits, since it is unlikely that a complete NP scenario would affect only one parameter while leaving the others unchanged. We therefore consider a fit varying simultaneously all the relevant 12 lepton-flavor-universal Wilson coefficients. This multidimensional fit also avoids the look-elsewhere effect, which can occur when making a selected choice of observables or when assuming a subset of specific new physics directions. The results are presented in Table VI. As can be seen, most primed coefficients (with right-handed quark currents) are only loosely constrained with the currently available data. In Table VII we compare the significance of different NP fits (all lepton-flavor universal) compared to the SM and to each other considering the Wilks theorem [78]. Since the NP scenarios in Table VII are nested in the model of the next row, we can calculate p-values using the Wilks theorem. The difference in χ^2 between the two models is itself a χ^2 distribution with a number of degrees of freedom equal to the difference in the number of parameters. The p value therefore indicates the significance of the new parameters added. We have then converted these p values to sigmas. From Table VII, it is clear that the main coefficient explaining the measured tensions in $b \to s$ decays is C_9 and beyond that adding further degrees of freedom does not improve the fit significantly. Thus, also the Wilks test

TABLE V. Two-operator NP fits to all observables (post-$R_{K^{(*)}}$ update). The corresponding plots are given in Fig. 2.

All observables post-$R_{K^{(*)}}$ update ($\chi^2_{\rm SM} = 271.0$)			
	Best-fit value	$\chi^2_{\rm min}$	Pull$_{\rm SM}$
$\{\delta C^{\mu}_9, \delta C^{e}_9\}$	$\{-0.96 \pm 0.13, -0.74 \pm 0.21\}$	228.8	6.2σ
$\{\delta C^{\mu}_{10}, \delta C^{e}_{10}\}$	$\{0.15 \pm 0.15, -0.03 \pm 0.21\}$	268.3	1.1σ
$\{\delta C^{\mu}_9, \delta C^{\mu}_{10}\}$	$\{-0.78 \pm 0.12, -0.19 \pm 0.10\}$	237.2	5.5σ
$\{\delta C_9, \delta C_{10}\}$	$\{-0.97 \pm 0.13, 0.09 \pm 0.15\}$	230.3	6.0σ

TABLE VI. The 12-dimensional (lepton-flavor-universal) fit to all observables.

All observables with $\chi^2_{\rm SM} = 271.0$ post-$R_{K^{(*)}}$ update ($\chi^2_{\rm min} = 222.5$; Pull$_{\rm SM} = 4.7\sigma$)			
δC_7		δC_8	
0.07 ± 0.03		-0.70 ± 0.50	
$\delta C'_7$		$\delta C'_8$	
-0.01 ± 0.01		-0.50 ± 1.20	
δC_9	$\delta C'_9$	δC_{10}	$\delta C'_{10}$
-1.18 ± 0.19	0.06 ± 0.31	0.23 ± 0.20	-0.05 ± 0.19
C_{Q_1}	C'_{Q_1}	C_{Q_2}	C'_{Q_2}
-0.30 ± 0.14	-0.18 ± 0.14	0.01 ± 0.02	-0.03 ± 0.07

TABLE VII. Pull$_{\rm SM}$ of 1-, 2-, 4-, 6-, and 12-dimensional fit. The last row includes all Wilson coefficients (WCs) including the chirality-flipped primed coefficients. The last column indicates the significance of the improvement of the fit compared to the previous row.

All observables (post-$R_{K^{(*)}}$ update)				
Set of WCs	Param	$\chi^2_{\rm min}$	Pull$_{\rm SM}$	Improvement
SM	0	271.0	⋯	⋯
C_9	1	230.7	6.3σ	6.3σ
C_9, C_{10}	2	230.3	6.0σ	0.6σ
C_7, C_8, C_9, C_{10}	4	225.3	5.9σ	1.7σ
$C_7, C_8, C_9, C_{10}, C_{Q_1}, C_{Q_2}$	6	224.7	5.6σ	0.3σ
All WCs (including primed)	12	222.5	4.7σ	0.1σ

confirms the crucial role of C_9 for the explanation of the anomalies in the angular observables and branching ratios.

IV. SUMMARY

In light of the recent LHCb measurement of R_K and R_{K^*}, which is in agreement with the Standard Model prediction, we have analyzed the current status of $b \to s$ semileptonic decays, including this new measurement, as well as the very recent measurement of R_K and $\mathrm{BR}(B^+ \to K^+\mu^+\mu^-)$ by the CMS Collaboration. We have also updated the CKM parameters to the PDG 2022 values.

The clean observables R_K, R_{K^*}, and $\mathrm{BR}(B_s \to \mu^+\mu^-)$ are now all in good agreement with the SM. The ratios constrain new physics contributions in $b \to s\ell^+\ell^-$ decays to be lepton-flavor universal, with room for only small universality violating contributions, while $\mathrm{BR}(B_s \to \mu^+\mu^-)$ constrains new physics contributions in the axial Wilson coefficient C_{10}. Furthermore, we showed that, although the two-dimensional fit $\{C_9^\mu, C_{10}^\mu\}$ (with C_9^e and C_{10}^e kept to their SM values) indicates preference for NP in C_9^μ and to a lesser degree in C_{10}^μ, this two-operator fit should be viewed critically because it gives a LFUV solution that is at odds with the recent $R_{K^{(*)}}$ measurements.

However, the tensions in the angular observables and branching ratios are untouched by the new LHCb measurements. These tensions are best explained by a lepton-flavor-universal NP in the Wilson coefficient C_9, which is mostly due to the low-q^2 observables, especially from the [6–8] GeV^2 bin, keeping in mind that this latter one, on the one hand, is more sensitive to C_9 contributions and, on the other hand, more prone to being contaminated by charm-loop contributions. Moreover, as shown via the Wilks test, new physics contributions in C_9 is the main scenario explaining the measured tensions in $b \to s$ decays and there is no significant improvement in the fit when considering more complex models with additional degrees of freedom.

ACKNOWLEDGMENTS

The authors are grateful to P. Owen for useful discussions. T. H. is supported by the Cluster of Excellence "Precision Physics, Fundamental Interactions, and Structure of Matter" (PRISMA$^+$ EXC 2118/1) funded by the German Research Foundation (DFG) within the German Excellence Strategy (Project ID 39083149). The work of S. N. was supported in part by the INFN research initiative Exploring New Physics (ENP).

---

[1] LHCb Collaboration, Test of lepton universality with $B^0 \to K^{*0}\ell^+\ell^-$ decays, J. High Energy Phys. 08 (2017) 055.

[2] LHCb Collaboration, Test of lepton universality in beauty-quark decays, Nat. Phys. **18**, 277 (2022).

[3] G. Hiller and F. Kruger, More model-independent analysis of $b \to s$ processes, Phys. Rev. D **69**, 074020 (2004).

[4] M. Bordone, G. Isidori, and A. Pattori, On the standard model predictions for R_K and R_{K^*}, Eur. Phys. J. C **76**, 440 (2016).

[5] LHCb Collaboration, Measurement of form-factor-independent observables in the decay $B^0 \to K^{*0}\mu^+\mu^-$, Phys. Rev. Lett. **111**, 191801 (2013).

[6] LHCb Collaboration, Differential branching fractions and isospin asymmetries of $B \to K^{(*)}\mu^+\mu^-$ decays, J. High Energy Phys. 06 (2014) 133.

[7] LHCb Collaboration, Differential branching fraction and angular analysis of $\Lambda_b^0 \to \Lambda\mu^+\mu^-$ decays, J. High Energy Phys. 06 (2015) 115.

[8] LHCb Collaboration, Angular analysis and differential branching fraction of the decay $B_s^0 \to \phi\mu^+\mu^-$, J. High Energy Phys. 09 (2015) 179.

[9] LHCb Collaboration, Angular analysis of the $B^0 \to K^{*0}\mu^+\mu^-$ decay using 3 fb^{-1} of integrated luminosity, J. High Energy Phys. 02 (2016) 104.

[10] LHCb Collaboration, Measurement of CP-averaged observables in the $B^0 \to K^{*0}\mu^+\mu^-$ decay, Phys. Rev. Lett. **125**, 011802 (2020).

[11] LHCb Collaboration, Angular analysis of the $B^+ \to K^{*+}\mu^+\mu^-$ decay, Phys. Rev. Lett. **126**, 161802 (2021).

[12] LHCb Collaboration, Angular analysis of the rare decay $B_s^0 \to \phi\mu^+\mu^-$, J. High Energy Phys. 11 (2021) 043.

[13] LHCb Collaboration, Branching fraction measurements of the rare $B_s^0 \to \phi\mu^+\mu^-$ and $B_s^0 \to f_2'(1525)\mu^+\mu^-$- decays, Phys. Rev. Lett. **127**, 151801 (2021).

[14] S. Descotes-Genon, J. Matias, and J. Virto, Understanding the $B \to K^*\mu^+\mu^-$ anomaly, Phys. Rev. D **88**, 074002 (2013).

[15] W. Altmannshofer and D. M. Straub, New physics in $B \to K^*\mu\mu$?, Eur. Phys. J. C **73**, 2646 (2013).

[16] F. Beaujean, C. Bobeth, and D. van Dyk, Comprehensive Bayesian analysis of rare (semi)leptonic and radiative B decays, Eur. Phys. J. C **74**, 2897 (2014).

[17] R. R. Horgan, Z. Liu, S. Meinel, and M. Wingate, Calculation of $B^0 \to K^{*0}\mu^+\mu^-$ and $B_s^0 \to \phi\mu^+\mu^-$ observables using form factors from lattice QCD, Phys. Rev. Lett. **112**, 212003 (2014).

[18] T. Hurth and F. Mahmoudi, On the LHCb anomaly in $B \to K^*\ell^+\ell^-$, J. High Energy Phys. 04 (2014) 097.

[19] C. Bobeth, M. Chrzaszcz, D. van Dyk, and J. Virto, Long-distance effects in $B \to K^*\ell\ell$ from analyticity, Eur. Phys. J. C **78**, 451 (2018).

[20] N. Gubernari, D. van Dyk, and J. Virto, Non-local matrix elements in $B_{(s)} \to \{K^{(*)}, \phi\}\ell^+\ell^-$, J. High Energy Phys. 02 (2021) 088.

[21] N. Gubernari, M. Reboud, D. van Dyk, and J. Virto, Improved theory predictions and global analysis of exclusive $b \to s\mu^+\mu^-$ processes, J. High Energy Phys. 09 (2022) 133.

[22] R. Alonso, B. Grinstein, and J. Martin Camalich, $SU(2) \times U(1)$ gauge invariance and the shape of new physics in rare B decays, Phys. Rev. Lett. **113**, 241802 (2014).

[23] G. Hiller and M. Schmaltz, R_K and future $b \to s\ell\ell$ physics beyond the standard model opportunities, Phys. Rev. D **90**, 054014 (2014).

[24] D. Ghosh, M. Nardecchia, and S. A. Renner, Hint of lepton flavour non-universality in B meson decays, J. High Energy Phys. 12 (2014) 131.

[25] S. Biswas, D. Chowdhury, S. Han, and S. J. Lee, Explaining the lepton non-universality at the LHCb and CMS within a unified framework, J. High Energy Phys. 02 (2015) 142.

[26] T. Hurth, F. Mahmoudi, and S. Neshatpour, Global fits to $b \to s\ell\ell$ data and signs for lepton non-universality, J. High Energy Phys. 12 (2014) 053.

[27] W. Altmannshofer and D. M. Straub, New physics in $b \to s$ transitions after LHC run 1, Eur. Phys. J. C **75**, 382 (2015).

[28] G. Hiller and M. Schmaltz, Diagnosing lepton-nonuniversality in $b \to s\ell\ell$, J. High Energy Phys. 02 (2015) 055.

[29] D. Bečirević, S. Fajfer, and N. Košnik, Lepton flavor nonuniversality in $b \to s\ell^+\ell^-$ processes, Phys. Rev. D **92**, 014016 (2015).

[30] S. Descotes-Genon, L. Hofer, J. Matias, and J. Virto, Global analysis of $b \to s\ell\ell$ anomalies, J. High Energy Phys. 06 (2016) 092.

[31] T. Hurth, F. Mahmoudi, and S. Neshatpour, On the anomalies in the latest LHCb data, Nucl. Phys. **B909**, 737 (2016).

[32] LHCb Collaboration, Test of lepton universality using $B^+ \to K^+\ell^+\ell^-$ decays, Phys. Rev. Lett. **113**, 151601 (2014).

[33] W. Altmannshofer, C. Niehoff, P. Stangl, and D. M. Straub, Status of the $B \to K^*\mu^+\mu^-$ anomaly after Moriond 2017, Eur. Phys. J. C **77**, 377 (2017).

[34] B. Capdevila, A. Crivellin, S. Descotes-Genon, J. Matias, and J. Virto, Patterns of new physics in $b \to s\ell^+\ell^-$ transitions in the light of recent data, J. High Energy Phys. 01 (2018) 093.

[35] G. D'Amico, M. Nardecchia, P. Panci, F. Sannino, A. Strumia, R. Torre, and A. Urbano, Flavour anomalies after the R_{K^*} measurement, J. High Energy Phys. 09 (2017) 010.

[36] M. Ciuchini, A. M. Coutinho, M. Fedele, E. Franco, A. Paul, L. Silvestrini, and M. Valli, On flavourful Easter eggs for new physics hunger and lepton flavour universality violation, Eur. Phys. J. C **77**, 688 (2017).

[37] L.-S. Geng, B. Grinstein, S. Jäger, J. Martin Camalich, X.-L. Ren, and R.-X. Shi, Towards the discovery of new physics with lepton-universality ratios of $b \to s\ell\ell$ decays, Phys. Rev. D **96**, 093006 (2017).

[38] A. K. Alok, B. Bhattacharya, A. Datta, D. Kumar, J. Kumar, and D. London, New physics in $b \to s\mu^+\mu^-$ after the measurement of R_{K^*}, Phys. Rev. D **96**, 095009 (2017).

[39] T. Hurth, F. Mahmoudi, D. Martinez Santos, and S. Neshatpour, Lepton nonuniversality in exclusive $b \to s\ell\ell$ decays, Phys. Rev. D **96**, 095034 (2017).

[40] A. Arbey, T. Hurth, F. Mahmoudi, and S. Neshatpour, Hadronic and new physics contributions to $b \to s$ transitions, Phys. Rev. D **98**, 095027 (2018).

[41] M. Algueró, B. Capdevila, A. Crivellin, S. Descotes-Genon, P. Masjuan, J. Matias, and J. Virto, Emerging patterns of new physics with and without lepton flavour universal contributions, Eur. Phys. J. C **79**, 714 (2019).

[42] A. K. Alok, A. Dighe, S. Gangal, and D. Kumar, Continuing search for new physics in $b \to s\mu\mu$ decays: Two operators at a time, J. High Energy Phys. 06 (2019) 089.

[43] A. Datta, J. Kumar, and D. London, The B anomalies and new physics in $b \to se^+e^-$, Phys. Lett. B **797**, 134858 (2019).

[44] J. Aebischer, W. Altmannshofer, D. Guadagnoli, M. Reboud, P. Stangl, and D. M. Straub, B-decay discrepancies after Moriond 2019, Eur. Phys. J. C **80**, 252 (2020).

[45] A. Arbey, T. Hurth, F. Mahmoudi, D. Martínez Santos, and S. Neshatpour, Update on the $b \to s$ anomalies, Phys. Rev. D **100**, 015045 (2019).

[46] R.-X. Shi, L.-S. Geng, B. Grinstein, S. Jäger, and J. Martin Camalich, Revisiting the new-physics interpretation of the $b \to c\tau\nu$ data, J. High Energy Phys. 12 (2019) 065.

[47] A. K. Alok, S. Kumbhakar, and S. Uma Sankar, A unique discrimination between new physics scenarios in $b \to s\mu^+\mu^-$ anomalies, Eur. Phys. J. Plus **137**, 354 (2022).

[48] T. Hurth, F. Mahmoudi, and S. Neshatpour, Implications of the new LHCb angular analysis of $B \to K^*\mu^+\mu^-$: Hadronic effects or new physics?, Phys. Rev. D **102**, 055001 (2020).

[49] M. Ciuchini, M. Fedele, E. Franco, A. Paul, L. Silvestrini, and M. Valli, Lessons from the $B^{0,+} \to K^{*0,+}\mu^+\mu^-$ angular analyses, Phys. Rev. D **103**, 015030 (2021).

[50] D. Bečirević, F. Jaffredo, A. Peñuelas, and O. Sumensari, New Physics effects in leptonic and semileptonic decays, J. High Energy Phys. 05 (2021) 175.

[51] T. Hurth, F. Mahmoudi, and S. Neshatpour, Model independent analysis of the angular observables in $B^0 \to K^{*0}\mu^+\mu^-$ and $B^+ \to K^{*+}\mu^+\mu^-$, Phys. Rev. D **103**, 095020 (2021).

[52] L.-S. Geng, B. Grinstein, S. Jäger, S.-Y. Li, J. Martin Camalich, and R.-X. Shi, Implications of new evidence for lepton-universality violation in $b \to s\ell + \ell$- decays, Phys. Rev. D **104**, 035029 (2021).

[53] W. Altmannshofer and P. Stangl, New physics in rare B decays after Moriond 2021, Eur. Phys. J. C **81**, 952 (2021).

[54] M. Algueró, B. Capdevila, S. Descotes-Genon, J. Matias, and M. Novoa-Brunet, $b \to s\ell^+\ell^-$ global fits after R_{K_S} and $R_{K^{*+}}$, Eur. Phys. J. C **82**, 326 (2022).

[55] T. Hurth, F. Mahmoudi, D. M. Santos, and S. Neshatpour, More indications for lepton nonuniversality in $b \to s\ell^+\ell^-$, Phys. Lett. B **824**, 136838 (2022).

[56] CMS Collaboration, Measurement of the $B_S^0 \to \mu^+\mu^-$ decay properties and search for the $B^0 \to \mu^+\mu^-$ decay in proton-proton collisions at $\sqrt{s} = 13$ TeV, Phys. Lett. B **842**, 137955 (2023).

[57] ATLAS Collaboration, Study of the rare decays of B_s^0 and B^0 mesons into muon pairs using data collected during 2015 and 2016 with the ATLAS detector, J. High Energy Phys. 04 (2019) 098.

[58] LHCb Collaboration, Measurement of the $B_s^0 \to \mu^+\mu^-$ decay properties and search for the $B^0 \to \mu^+\mu^-$ and $B_s^0 \to \mu^+\mu^-\gamma$ decays, Phys. Rev. D **105**, 012010 (2022).
[59] LHCb Collaboration, Analysis of neutral B-meson decays into two muons, Phys. Rev. Lett. **128**, 041801 (2022).
[60] S. Neshatpour, T. Hurth, F. Mahmoudi, and D. Martinez Santos, Neutral current B-decay anomalies, Springer Proc. Phys. **292**, 11 (2023).
[61] LHCb Collaboration, Measurement of lepton universality parameters in $B^+ \to K^+\ell^+\ell^-$ and $B^0 \to K^{*0}\ell^+\ell^-$ decays, Phys. Rev. D **108**, 032002 (2023).
[62] CMS Collaboration, Test of lepton flavor universality in $B^\pm \to K^\pm\ell^+\ell^-$ decays Report No. CMS-PAS-BPH-22-005.
[63] Particle Data Group Collaboration, Review of particle physics, Prog. Theor. Exp. Phys. **2020**, 083C01 (2020).
[64] Particle Data Group Collaboration, Review of particle physics, Prog. Theor. Exp. Phys. **2022**, 083C01 (2022).
[65] F. Mahmoudi, SuperIso: A program for calculating the isospin asymmetry of $B \to K^*\gamma$ in the MSSM, Comput. Phys. Commun. **178**, 745 (2008).
[66] F. Mahmoudi, SuperIso v2.3: A program for calculating flavor physics observables in supersymmetry, Comput. Phys. Commun. **180**, 1579 (2009).
[67] F. Mahmoudi, SuperIso v3.0, flavor physics observables calculations: Extension to NMSSM, Comput. Phys. Commun. **180**, 1718 (2009).
[68] S. Neshatpour and F. Mahmoudi, Flavour physics with SuperIso, Proc. Sci. TOOLS2020 (**2021**) 036 [arXiv:2105.03428].
[69] S. Neshatpour and F. Mahmoudi, Flavour physics phenomenology with SuperIso, Proc. Sci. CompTools2021 (**2022**) 010 [arXiv:2207.04956].
[70] M. Algueró, A. Biswas, B. Capdevila, S. Descotes-Genon, J. Matias, and M. Novoa-Brunet, To (b)e or not to (b)e: No electrons at LHCb, Eur. Phys. J. C **83**, 648 (2023).
[71] M. Ciuchini, M. Fedele, E. Franco, A. Paul, L. Silvestrini, and M. Valli, Constraints on lepton universality violation from rare B decays, Phys. Rev. D **107**, 055036 (2023).
[72] A. Greljo, J. Salko, A. Smolkovič, and P. Stangl, Rare b decays meet high-mass Drell-Yan, J. High Energy Phys. 05 (2023) 087.
[73] N. R. Singh Chundawat, CP violation in $b \to s\ell\ell$: A model independent analysis, Phys. Rev. D **107**, 075014 (2023).
[74] LHCb Collaboration, Tests of lepton universality using $B^0 \to K_S^0\ell^+\ell^-$ and $B^+ \to K^{*+}\ell^+\ell^-$ decays, Phys. Rev. Lett. **128**, 191802 (2022).
[75] P. Owen (private communication).
[76] C. Bobeth, G. Hiller, and D. van Dyk, The benefits of $\bar{B} \to \bar{K}^* l^+ l^-$ decays at low recoil, J. High Energy Phys. 07 (2010) 098.
[77] M. Beylich, G. Buchalla, and T. Feldmann, Theory of $B \to K^{(*)}\ell^+\ell^-$ decays at high q^2: OPE and quark-hadron duality, Eur. Phys. J. C **71**, 1635 (2011).
[78] S. S. Wilks, The large-sample distribution of the likelihood ratio for testing composite hypotheses, Ann. Math. Stat. **9**, 60 (1938).